

Two-loop renormalization of the Pontryagin density in pure Yang-Mills theory

Pyungwon Ko* and Taehoon Lee

Department of Physics, Seoul National University, Seoul 151, Korea

(Received 1 June 1987)

Two-loop renormalization of the Pontryagin density in pure Yang-Mills theory is studied in the Feynman gauge. Dimensional regularization is assumed. Our calculation supports the expression $(g_B^2 Z_3 / 32\pi^2) *F^{\mu\nu\alpha} F_{\mu\nu}^{\alpha}$, with $F_{\mu\nu}^a = \partial_\mu A_\nu^a - \partial_\nu A_\mu^a + g_B Z_3^{1/2} f_{abc} A_\mu^b A_\nu^c$, as the correct renormalized Pontryagin density.

It is well known¹ that the term proportional to the Pontryagin density is needed in the effective Lagrangian density of the quantized Yang-Mills theory because of the topologically nontrivial vacuum structure. Since the space-time integral of the Pontryagin density is a topological invariant (at least in the classical sense), one would naturally expect that the Pontryagin density be renormalized fully by wave-function renormalization of Yang-Mills (YM) gauge fields ($A_\mu^a \rightarrow Z_3^{1/2} A_\mu^a$) and the coupling-constant renormalization ($g \rightarrow g_B$). Despite some doubt concerning whether such a topology-based argument can be trusted in renormalized perturbation theory, this strongly suggests the renormalized Pontryagin density of the form

$$\mathcal{W}(A) = \frac{g_B^2 Z_3}{32\pi^2} *F^{\mu\nu\alpha} F_{\mu\nu}^{\alpha}, \tag{1}$$

where $*F^{\mu\nu\alpha} = \frac{1}{2} \epsilon^{\mu\nu\alpha\beta} F_{\alpha\beta}^a$ and

$$F_{\mu\nu}^a = \partial_\mu A_\nu^a - \partial_\nu A_\mu^a + g_B Z_3^{1/2} f_{abc} A_\mu^b A_\nu^c. \tag{2}$$

Some time ago Jones and Leveille² verified, by explicit Feynman-diagram calculations, the one-loop finiteness of the amplitude including an insertion of the renormalized Pontryagin density as given in Eq. (1).

We now have two versions of proof, which *directly*³ assert all-order finiteness of vertex functions including an insertion of the renormalized Pontryagin density (1). The proof given by the authors in Ref. 4 was based on the background-gauge background-field method, while the authors in Ref. 5 resorted to the anomalous $U_A(1)$ Ward-Takahashi identity (in the context of QCD). But one may suspect whether the arguments of Ref. 4, which depend rather crucially on the special characters of the background-gauge background-field method, will also apply, say, when a more usual covariant gauge is as-

sumed. On the other hand, the proof of Ref. 5 (which is addressed in usual covariant gauges) is restricted to the case when there exist some fermion fields, and therefore does not directly apply to pure YM theory. Also, the appearance of the four-dimensional pseudotensor $\epsilon^{\mu\nu\lambda\delta}$ in the Pontryagin density casts some doubt (especially if one has the popular dimensional-regularization scheme in mind) on whether various symmetry restrictions can be consistently imposed as needed in the arguments of these authors.

Under the circumstances, we have felt that it should be worth checking the assertion by explicit two-loop calculations in the context of pure YM theory in the Feynman gauge and assuming dimensional regularization. This short paper reports our findings. We have followed Jones and Leveille² in the treatment of the pseudotensor $\epsilon^{\mu\nu\lambda\delta}$ in dimensional regularization; viz., $\epsilon^{\mu\nu\lambda\delta}$ ($\mu, \nu, \lambda, \delta = 0, 1, \dots, n-1$) is totally antisymmetric and can be identified with $\text{const} \times \text{Tr}(\gamma_5 \gamma^\mu \gamma^\nu \gamma^\lambda \gamma^\delta)$ where γ_5 and γ^μ in n dimensions are defined consistently with the relation $\text{Tr}(\gamma_5 \gamma^\mu \gamma^\nu) = 0$. (The 't Hooft-Veltman γ_5 prescription,⁶ which is known to be unambiguous, is one consistent realization of this.) Our calculation confirms that the expression (1), solely on the basis of the renormalization counterterms as given in the expression (and no further counterterm), indeed leads to two-loop finite (off-shell) matrix elements.

The authors in Ref. 2 verified that, with a single insertion of the operator $\mathcal{W}(A)$, the one-loop amplitude with two external YM vector legs is finite. In this paper we shall also look at the corresponding amplitude with three external YM vector legs, and then go on to verify the finiteness of the two-loop amplitude with two external YM vector legs. Including the source term for the Pontryagin density operator, the renormalized effective Lagrangian density of YM theory in the Feynman gauge reads

$$\begin{aligned} \mathcal{L}_{\text{eff}}(x) = & -\frac{1}{4} Z_3 F^{\mu\nu a}(x) F_{\mu\nu}^a(x) - \frac{1}{2} [\partial^\mu A_\mu^a(x)]^2 - \bar{Z}_3 \bar{\chi}^a(x) \partial^\mu [\partial_\mu \delta_{ac} + g_B Z_3^{1/2} f_{abc} A_\mu^b(x)] \chi^c(x) \\ & + \Theta(x) \frac{g_B^2 Z_3}{32\pi^2} *F^{\mu\nu\alpha}(x) F_{\mu\nu}^{\alpha}(x), \end{aligned} \tag{3}$$

where $F^{\mu\nu a}$ is given in Eq. (2), $(\chi^a, \bar{\chi}^a)$ represent Faddeev-Popov ghost fields with the corresponding wave-function renormalization constant \bar{Z}_3 , and we have written

$$g_B = Z_1 Z_3^{-3/2} g \quad (g = \text{renormalized coupling constant}). \quad (4)$$

The renormalization constants, to the order we need for our calculations, are given explicitly as⁷

$$Z_3 = 1 + \frac{g^2 C_2(G)}{(4\pi)^2} \frac{5}{3\epsilon} + \frac{g^4 [C_2(G)]^2}{(4\pi)^4} \left[-\frac{25}{12} \frac{1}{\epsilon^2} + \frac{23}{8} \frac{1}{\epsilon} \right] + \dots, \quad (5a)$$

$$Z_1 = 1 + \frac{g^2 C_2(G)}{(4\pi)^2} \frac{2}{3\epsilon} + \frac{g^4 [C_2(G)]^2}{(4\pi)^4} \left[-\frac{13}{8} \frac{1}{\epsilon^2} + \frac{71}{48} \frac{1}{\epsilon} \right] + \dots, \quad (5b)$$

$$\bar{Z}_3 = 1 + \dots, \quad (5c)$$

where $f^{acd} f^{bcd} = C_2(G) \delta^{ab}$ and $\epsilon = 2 - n/2$. Momentum-space Feynman rules associated with the vertex insertion of the operator $\mathcal{W}(A)$ are shown in Fig. 1. [The symbol \square denotes the $\mathcal{W}(A)$ insertion with $(g_B = g, Z_3 = 1)$, and the symbol \boxtimes denotes the corresponding counterterm contribution as implied by Eq. (1).] Note that $\mathcal{W}(A)$, being equal to

$$2 \frac{g_B^2 Z_3}{32\pi^2} \partial_\mu \epsilon^{\mu\nu\lambda\delta} (A_\nu^a \partial_\lambda A_\delta^a + \frac{1}{3} g_B Z_3^{1/2} f_{abc} A_\nu^a A_\lambda^b A_\delta^c),$$

does not contain any quartic piece in A_μ^a .

We have first studied one-loop amplitudes which contain a $\mathcal{W}(A)$ insertion and involve three external (amputated) YM vector legs. Relevant Feynman diagrams are shown in Fig. 2. When we denote this vertex function, renormalized as indicated by the form (1), by

$$F^{(1)}(p, q, r)_{\mu\nu\alpha}^{abc} = K \frac{g^3}{64\pi^2} 8i f^{abc} \epsilon_{\mu\nu\alpha\beta} (p + q + r)^\beta \times \frac{g^2 C_2(G)}{(4\pi)^2} \frac{1}{2\epsilon} + (\text{finite terms}), \quad (6)$$

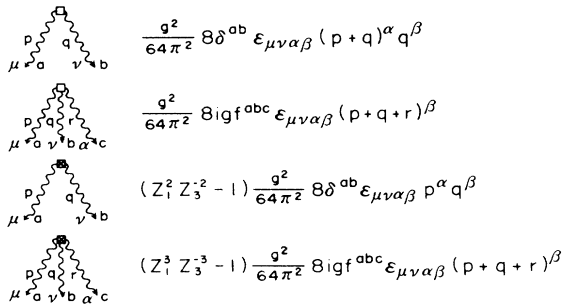


FIG. 1. Feynman rules associated with the $\mathcal{W}(A)$ -vertex insertion.

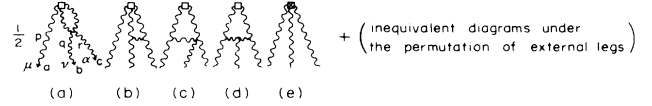


FIG. 2. One-loop diagrams with three external YM vector legs associated with the $\mathcal{W}(A)$ -vertex insertion.

our calculation shows that diagrams of the type in Figs. 2(a)–2(e) contribute, respectively, the values -9 , $\frac{9}{2}$, $\frac{27}{2}$, -3 , and -6 to K . They clearly sum up to $K = 0$, thus confirming that the amplitude $F^{(1)}(p, q, r)_{\mu\nu\alpha}^{abc}$ is indeed ultraviolet finite. Note that corresponding one-loop amplitudes with four external YM vector legs are power-counting finite since one momentum factor from the $\mathcal{W}(A)$ insertion is really an external one.

We now turn to the analysis of corresponding two-loop diagrams, restricting our attention to those with only two external YM vector legs. For this consideration, we have found that the exact expression⁸ for the one-loop renormalized YM vector propagator,

$$-i \delta^{ab} \left[\frac{\eta^{\mu\nu}}{p^2} - \frac{p^\mu p^\nu}{(p^2)^2} \right] \frac{g^2 C_2(G)}{(4\pi)^2} \frac{5}{3} \times \left[\Gamma(\epsilon) \left(1 + \frac{31}{15} \epsilon \right) \left[-\frac{p^2}{4\pi\mu^2} \right]^{-\epsilon} - \frac{1}{\epsilon} \right], \quad (7)$$

is very useful. (Diagrammatically, this one-loop renormalized vector propagator will be represented as in Fig. 3.) In Fig. 4 we have given all relevant two-loop Feynman diagrams, grouped appropriately for conveniences in calculation. This two-loop amplitude may be represented as

$$F^{(2)}(p, q)_{\mu\nu}^{ab} = (p + q)^\alpha L^{(2)}(p, q)_{\mu\nu\alpha}^{ab} \quad (8)$$

with

$$L^{(2)}(p, q)_{\mu\nu\alpha}^{ab} = -\frac{g^2}{64\pi^2} 8\delta^{ab} \epsilon_{\mu\nu\alpha\beta} p^\beta A(p, q), \quad (9)$$

where $A(p, q)$ is a Lorentz scalar. In Eq. (8) we have explicitly factored out one external momentum $(p + q)^\alpha$ originating from the $\mathcal{W}(A)$ vertex. [Note that $\mathcal{W}(A)$ corresponds to a total derivative.] The function $A(p, q)$ in Eq. (9), once all one-loop subgraph divergences have been taken care of, will be at most logarithmically divergent by power counting. Being only logarithmically divergent, it should thus be sufficient for us to verify the



FIG. 3. One-loop renormalized YM vector propagator.

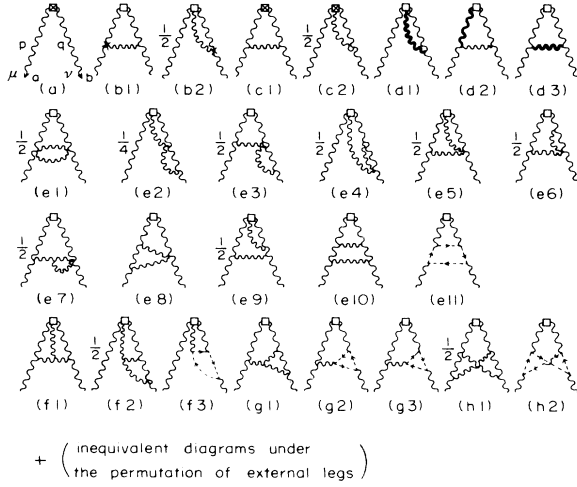


FIG. 4. Two-loop diagrams with two external YM vector legs associated with the $\mathcal{W}(A)$ -vertex insertion.

finiteness of, say, $A(p, q = -p)$ to demonstrate the ultraviolet finiteness of the function $F^{(2)}(p, q)_{\mu\nu}^{ab}$. This is precisely the procedure we have adopted here: look into the finiteness of $A(p, -p)$. (Actually, with $q = -p$, tadpolelike diagrams as shown in Fig. 5 vanish identically in dimensional regularization. By this reason we have not included such tadpolelike diagrams in Fig. 4.)

Here a brief explanation on the nature of various two-loop diagrams shown in Fig. 4 should be useful. The diagram in Fig. 4(a) represents the two-loop counterterm contribution coming from the operator $\mathcal{W}(A)$ and is proportional to $(Z_1^2 Z_3^{-2} - 1)^2$ loop. Diagrams in Figs. 4(b) and 4(c) are those containing one-loop counterterms, while diagrams in Fig. 4(d) involve a one-loop renormalized vector propagator (see Fig. 3) as subdiagrams. It is relatively easy to identify divergent pieces from these diagrams. We obtain the following (divergent) contributions from them to the amplitude $A(p, -p)$:

$$\begin{aligned}
 \text{(i)} \quad & \int \frac{d^n k d^n l}{(2\pi)^{2n}} \frac{1}{k^2 D} = -\frac{X}{(p^2)^2}, \\
 \text{(ii)} \quad & \int \frac{d^n k d^n l}{(2\pi)^{2n}} \frac{k^\alpha l^\mu l^\nu}{k^2 D} = \frac{1}{2} \epsilon X \frac{p^\alpha}{p^2} \eta^{\mu\nu}, \\
 \text{(iii)} \quad & \int \frac{d^n k d^n l}{(2\pi)^{2n}} \frac{k^\alpha l^\mu l^\nu l^\lambda}{k^2 D} = -\frac{1}{8} \epsilon X \frac{p^\alpha p^\mu}{p^2} \eta^{\nu\lambda} - \frac{1}{96} (1 + \frac{35}{6} \epsilon) X \eta^{\alpha\mu} \eta^{\nu\lambda} + (\text{permutations of indices } \mu, \nu, \text{ and } \lambda), \\
 \text{(iv)} \quad & \epsilon_{\alpha\beta\gamma\delta} \int \frac{d^n k d^n l}{(2\pi)^{2n}} \frac{k^\alpha l^\beta l^\mu l^\nu \cdot k}{k^2 D} = \epsilon_{\alpha\beta\gamma\delta} \left[\frac{1}{16} (1 + \frac{15}{2} \epsilon) X p^\alpha \eta^{\beta\mu} + \frac{1}{48} (1 + \frac{49}{6} \epsilon) X p^\beta \eta^{\gamma\mu} \right], \\
 \text{(v)} \quad & \int \frac{d^n k d^n l}{(2\pi)^{2n}} \frac{1}{D(l-k)^2} = -3(1+2\epsilon) \frac{X}{(p^2)^2}, \\
 \text{(vi)} \quad & \int \frac{d^n k d^n l}{(2\pi)^{2n}} \frac{k^\alpha}{D(l-k)^2} = \frac{3}{2} (1+2\epsilon) X \frac{p^\alpha}{(p^2)^2}, \\
 \text{(vii)} \quad & \int \frac{d^n k d^n l}{(2\pi)^{2n}} \frac{k^\alpha k^\beta}{D(l-k)^2} = \int \frac{d^n k d^n l}{(2\pi)^{2n}} \frac{k^\alpha l^\beta}{D(l-k)^2} = -\frac{4}{3} (1 + \frac{85}{24} \epsilon) X \frac{p^\alpha p^\beta}{(p^2)^2} + \frac{1}{12} (1 + \frac{44}{3} \epsilon) X \frac{\eta^{\alpha\beta}}{p^2},
 \end{aligned} \tag{12}$$

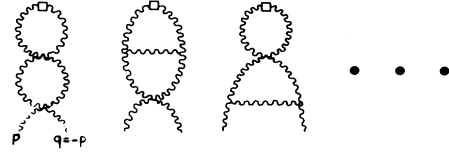


FIG. 5. Two-loop diagrams which vanish identically in dimensional regularization.

Diagrams	Contributions to $A(p, -p)$
Fig. 4(a)	$\frac{g^4 [C_2(G)]^2}{(4\pi)^4} \left[\frac{21}{4} \frac{1}{\epsilon^2} - \frac{67}{24} \frac{1}{\epsilon} \right]$
Figs. 4(b1) and 4(b2)	$g^4 [C_2(G)]^2 \left(\frac{14}{3} + 12\epsilon \right) Y$
Figs. 4(c1) and 4(c2)	$g^4 [C_2(G)]^2 (-1 - 6\epsilon) Y$
Figs. 4(d1)–4(d3)	$g^4 [C_2(G)]^2 \left[\left(\frac{85}{6} + \frac{3739}{36} \epsilon \right) X + \left(-\frac{85}{6} - \frac{130}{3} \epsilon \right) Y \right]$

(10)

Here, X and Y represent

$$\begin{aligned}
 X &= \frac{1}{(4\pi)^4} \frac{1}{2\epsilon^2} \left\{ 1 - \epsilon - 2\epsilon \left[\gamma + \ln \left[-\frac{p^2}{4\pi\mu^2} \right] \right] \right\}, \\
 Y &= \frac{1}{(4\pi)^4} \frac{1}{\epsilon^2} \left\{ 1 - \epsilon \left[\gamma + \ln \left[-\frac{p^2}{4\pi\mu^2} \right] \right] \right\},
 \end{aligned} \tag{11}$$

where μ is the normalization mass and γ is the Euler-Mascheroni constant.

Feynman diagrams shown in Figs. 4(e)–(h) are genuine two-loop diagrams, and identifying divergent pieces from them is nontrivial. For our purpose, we have found the integration formulas given in the Appendix of Ref. 2 quite useful. But the formulas given there are not sufficient, and we shall here give some additional integration formulas obtained by us. [The formula (i) below was obtained earlier in Ref. 9.] they are, up to finite contributions,

$$\begin{aligned}
\text{(viii)} \quad & \int \frac{d^n k d^n l}{(2\pi)^{2n}} \frac{k^\alpha k^\beta k^\gamma}{D(l-k)^2} = \int \frac{d^n k d^n l}{(2\pi)^{2n}} \frac{l^\alpha l^\beta k^\gamma}{D(l-k)^2} = \frac{5}{4} (1 + \frac{67}{15} \epsilon) X \frac{p^\alpha p^\beta p^\gamma}{(p^2)^2} - \frac{1}{24} (1 + \frac{44}{3} \epsilon) \frac{X}{p^2} (p^\alpha \eta^{\beta\gamma} + p^\beta \eta^{\gamma\alpha} + p^\gamma \eta^{\alpha\beta}), \\
\text{(ix)} \quad & \int \frac{d^n k d^n l}{(2\pi)^{2n}} \frac{l^\alpha l^\beta l^\gamma k^\mu}{D(l-k)^2} = -\frac{6}{5} (1 + \frac{1849}{360} \epsilon) X \frac{p^\alpha p^\beta p^\gamma p^\mu}{(p^2)^2} \\
& + \left[\frac{1}{80} (1 + \frac{241}{15} \epsilon) \frac{X}{p^2} (p^\alpha p^\beta \eta^{\gamma\mu} + p^\mu p^\alpha \eta^{\beta\gamma}) + \frac{3}{160} (1 + \frac{479}{135} \epsilon) X \eta^{\alpha\beta} \eta^{\gamma\mu} \right. \\
& \left. + (\text{permutations of indices } \alpha, \beta, \text{ and } \gamma) \right], \\
\text{(x)} \quad & \int \frac{d^n k d^n l}{(2\pi)^{2n}} \frac{l^\alpha l^\beta k^\gamma k^\mu}{D(l-k)^2} = -\frac{6}{5} (1 + \frac{1849}{360} \epsilon) X \frac{p^\alpha p^\beta p^\gamma p^\mu}{(p^2)^2} \\
& + \left[\frac{1}{80} (1 + \frac{241}{15} \epsilon) \frac{X}{p^2} (p^\alpha p^\beta \eta^{\gamma\mu} + p^\mu p^\alpha \eta^{\beta\gamma}) + (\text{permutations of indices } \alpha, \beta, \text{ and } \gamma) \right] \\
& + \frac{3}{80} (1 + \frac{179}{135} \epsilon) X \eta^{\alpha\beta} \eta^{\gamma\mu} + \frac{3}{80} (1 + \frac{629}{135} \epsilon) X (\eta^{\beta\gamma} \eta^{\alpha\mu} + \eta^{\gamma\alpha} \eta^{\beta\mu}),
\end{aligned}$$

where we have denoted $D = k^2(k+p)^2 l^2(l+p)^2(l-k)^2$ and followed the metric convention $(+1, -1, -1, \dots)$. Based on these formulas, the following (divergent) contributions to the amplitude $A(p, -p)$ have been obtained:

Diagrams	Contributions to $A(p, -p)$
Figs. 4(e1)–4(e4)	$g^4 [C_2(G)]^2 (-\frac{9}{4} - \frac{171}{8} \epsilon) X$
Figs. 4(e5) and 4(e6)	0
Figs. 4(e7)–4(e10)	$g^4 [C_2(G)]^2 (-\frac{41}{4} - \frac{433}{8} \epsilon) X$
Fig. 4(e11)	0
Figs. 4(f1)–4(f3)	$g^4 [C_2(G)]^2 (-\frac{23}{2} - \frac{251}{4} \epsilon) X$
Figs. 4(g1)–4(g3)	$g^4 [C_2(G)]^2 (\frac{113}{6} + \frac{2059}{18} \epsilon) X$
Figs. 4(h1) and 4(h2)	$g^4 [C_2(G)]^2 (\frac{3}{2} + \frac{43}{4} \epsilon) X$

(13)

The net contribution to $A(p, -p)$ from the terms shown in Eq. (10) is

$$\begin{aligned}
g^4 [C_2(G)]^2 \left[\frac{1}{(4\pi)^4} \left[\frac{21}{4} \frac{1}{\epsilon^2} - \frac{67}{24} \frac{1}{\epsilon} \right] - \left(\frac{21}{2} + \frac{112}{3} \epsilon \right) Y \right. \\
\left. + \left(\frac{85}{6} + \frac{3739}{36} \epsilon \right) X \right], \quad (14)
\end{aligned}$$

while that from the terms shown in Eq. (13) is

$$g^4 [C_2(G)]^2 \left[\left(\frac{21}{2} + \frac{363}{4} \epsilon \right) X - \left(\frac{85}{6} + \frac{3739}{36} \epsilon \right) X \right]. \quad (15)$$

Clearly, the two cancel. (Here note that the cancellation of nonpolynomial divergences, which of course follows from general renormalization theory, serves as a useful check of our calculation.) This way, we have explicitly verified that $A(p, -p)$ is indeed finite. The renormalized Pontryagin density, in the form given in Eq. (1), leads to a two-loop finite result.

We are very grateful to Professor C. Lee for suggesting the problem and useful discussions. This work was supported in part by the Daewoo Foundation and by the Korea Science and Engineering Foundation.

*Present address: Department of Physics, the University of Chicago, Chicago, Illinois 60637.

¹R. Jackiw and C. Rebbi, Phys. Rev. Lett. **37**, 172 (1976); C. Callan, R. Dashen, and D. Gross, Phys. Lett. **63B**, 334 (1976).

²D. R. T. Jones and J. P. Leveille, Nucl. Phys. **B206**, 473 (1982).

³By “directly” we here mean “without resorting to a topological reasoning” (which is rather uncertain in the context of renormalized perturbation theory).

⁴V. A. Novikov, M. A. Shifman, A. I. Vainshtein, and V. I. Zakharov (unpublished); P. Breitenlohner, D. Maison, and K. Stelle, Phys. Lett. **134B**, 63 (1984); K. S. Stelle, in *Supersymmetry, Supergravity and Related Topics*, proceedings of the

GIFT Seminar, Gerona, Spain, 1984, edited by F. Del Aguila, J. A. de Azcarraga, and L. E. Ibanez (World Scientific, Singapore, 1983).

⁵C. Lee and P. Y. Pac, Phys. Rev. D **33**, 2954 (1986).

⁶G. 't Hooft and M. Veltman, Nucl. Phys. **B44**, 189 (1972).

⁷D. R. T. Jones, Nucl. Phys. **B75**, 531 (1974); W. E. Caswell, Phys. Rev. Lett. **33**, 244 (1974); M. Calvo, Phys. Rev. D **15**, 730 (1977); O. V. Tarasov, A. A. Vladimirov, and A. Yu. Zharkov, Phys. Lett. **93B**, 429 (1980).

⁸P. Ramond, *Field Theory: A Modern Primer, Frontiers in Physics* (Lecture Note Series 51) (Benjamin Cummings, Reading, MA, 1981), p. 362.

⁹K. G. Chetyrkin, A. L. Kataev, and F. V. Tkachov, Phys. Lett. **85B**, 277 (1979).